Chapter IV

A Novel Measuring Circuit for Semiconductor Gas Sensors

The objective of this chapter is to analyze and investigate the effect of circuit components in the measuring circuit on gas sensing parameters. The parameters of interests are sensitivity, S and recovery time, t_r. Sensitivity relates closely to the sensing performance of gas sensors. While, recovery time indicates the speed of measuring. In general, sensitivity is defined as the ratio of the sensor resistance in air to the sensor resistance in gas ambient. Therefore, a circuit for determining an unknown resistance is needed. Moreover, recovery time is determined from the response curves obtained from the gas measuring circuit, cf. Fig. 3.13(b).

There are three basic circuits for calculating an unknown resistance as illustrated in Fig. 4.1: (a) constant current circuit, (b) voltage divider circuit (the conventional measuring circuit) and (c) constant voltage circuit. In this figure, the graphical current-voltage (I-V) characteristics with load line and the equations for calculating an unknown resistance are also given. Both of the constant current and the conventional circuit are commonly used to calculate the sensor resistance [14,68]. However, the constant current circuit is not suitable for practical applications since the common electrical source is the voltage source and the electrical loading effect seems to be critical due to high sensor resistance (ca. MΩ or more especially in air). In the case of the constant voltage circuit, it is rarely used, because the current measurement is not so preferable. Thus, for simplicity, the conventional circuit is generally employed to determined the sensor resistance.

The conventional circuit will perform its function correctly, if gas sensor acts as a linear resistive element. Unfortunately the real situation is much more complex, since the electrical properties of the potential barriers at the grain boundaries cause

this device to have a non-linear current-voltage (I-V) characteristics[1]. Consequently, it can be expected that the values of all external circuit components, i.e., series resistance, R and voltage source, V_{in} will affect the calculated sensor resistance and the calculated sensitivity. This critical situation makes the comparison of the sensitivity among different sensors impossible. Moreover, the equilibrium established between gas sensor and the external circuit components (the operating point) also controls the dynamic characteristics of gas sensor. The capacitance (C) at grain boundary also exhibits a voltage-dependent characteristic[1]. To overcome this problem, a thorough understanding of interactions between sensor characteristics and the measuring circuit is necessary.

In this chapter, an analysis and experiments have been done to clarify the effects of series resistance, R in the conventional measuring circuit on gas sensitivity and recovery time. In the experimental part, gas measuring circuit and various SnO_2 thick film gas sensors were employed to confirmed the analytical results. By considering the variation of the operating point of gas sensors in the conventional circuit, a novel measuring circuit with a fixed bias voltage was proposed to solve the problem found in the conventional circuit.

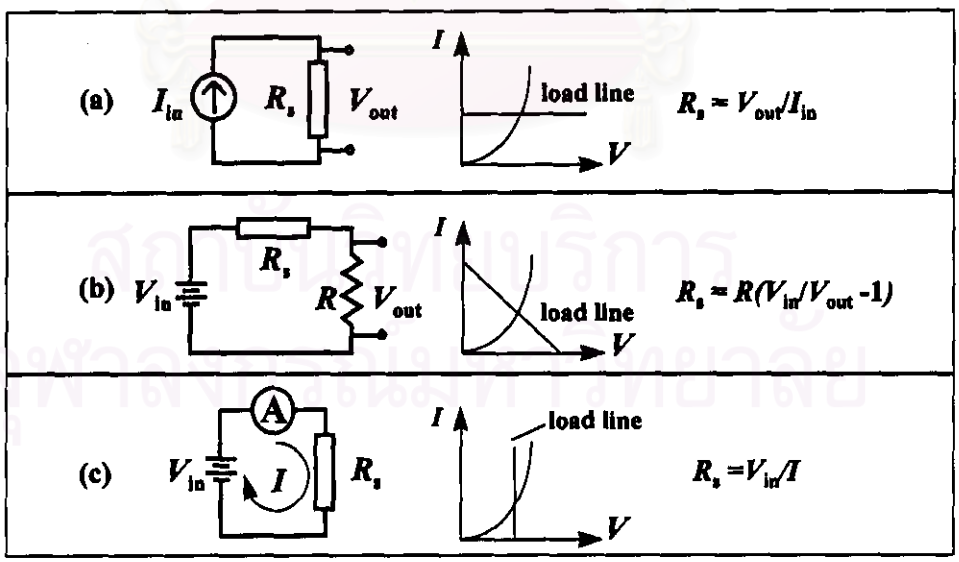

Fig. 4.1 Basic configuration circuits for measuring an unknown resistance; (a) constant current, (b) voltage divider and (c) constant voltage.

4.1 Analysis of Measuring Circuit

4.1.1 The Conventional Circuit

The conventional circuit is redrawn in Fig. 4.2(a). The sensor resistance, R_s can be calculated from the output voltage, V_{out} as shown in eq. (4.1).

$$R_s = R \cdot \left(\frac{V_{in}}{V_{out}} - 1 \right) \tag{4.1}$$

From the definition of sensitivity, the relation of sensitivity in terms of the output voltage can be derived as follows.

$$S = \frac{R_{air}}{R_{gas}} = \left(\frac{V_{in}/(V_{out\,in\,air}) - 1}{V_{in}/(V_{out\,in\,gas}) - 1} \right) = \left(\frac{V_{in}/(V_{in} - V_{air}) - 1}{V_{in}/(V_{in} - V_{gas}) - 1} \right) \tag{4.2}$$

Where V_{air} and V_{gas} are the voltage dropped across gas sensor in air and gas respectively. However, this equation does not show explicitly how S depends on the series resistance, R. This can be shown by considering the operating point of gas sensor using the load line concept. The load lines of the conventional circuit are also depicted in Fig 4.2(b) with *I-V* characteristics of gas sensor in air and gas ambient (reducing gas in this case). The load line equation can be written as follows.

$$I = \frac{V_{in}}{R} - \frac{V_s}{R} \tag{4.3}$$

Where I is the current flowing through the gas sensor and V_s is the voltage across the gas sensor. In this concept, gas sensors may behave as a linear or non-linear device. We may assume that I-V characteristic of gas sensor in air and gas can be expressed as eqs. (4.4) and (4.5).

$$I_{air} = f_{air}(V) \tag{4.4}$$

$$I_{gas} = f(V_{gas}) \tag{4.5}$$

Where $f(V)$ is a function representing the relation of current-voltage characteristic. If we know the certain relation of *I-V* characteristic, by solving eqs.

(4.3) to (4.5), V_{air} and V_{gas} in term of R and V_{in} can be obtained mathematically. Finally, S in function of R and V_{in} can be derived using eq. (4.2). It is known that I-V characteristic of gas sensors or other sintered ceramic devices may be described by the following empirical equation[1]

$$I = CV^{\alpha} \tag{4.6}$$

Where C is the proportional constant and α is the non-linear coefficient. The values of these parameters will be discussed in the section 4.3. It should be noted that if $\alpha = 1$, gas sensor will have a linear characteristic. The expression of S can be written in an alternative form by starting from eqs. (4.2) and (4.6).

$$S = \frac{C_{gas}}{C_{air}} \left(\frac{V_{gas}^{\alpha_{gas}-1}}{V_{air}^{\alpha_{air}-1}} \right) \tag{4.7}$$

In eq. (4.7), the subscripts air and gas show whether the parameters are in air or gas ambient. In the special case, I-V characteristic of gas sensor is a linear function, i.e., α_{air} and $\alpha_{gas} = 1$, hence eq. (4.7) can be reduced to the following form.

$$S = \frac{C_{gas}}{C_{air}} \tag{4.8}$$

It is clear that S will be constant and any change in R or V_{in} has no effect on S. In this case, the proportional constant, C is equivalent to the conductance of a gas sensor. However, in general case, where α_{air} or $\alpha_{gas} \neq 1$, S will depend on both R and V_{in}. As can be seen in eq. (4.7), the degree of dependency is determined heavily on the α parameter. From Fig. 4.2(b), it is clear that S changes with the variation of the slope of a load line, i.e., $1/R$. The same situation will occur, if V_{in} is changed. Thus, the careful selection of R and V_{in} are very important. The different bias conditions will lead to the difference of S and the comparison of gas sensing between various sensors will be impossible. Moreover, even though the same gas sensor is used, the different values of S will be obtained if it is characterized at different bias conditions (Fig. 4.7). This will be experimentally demonstrated in the section 4.3.

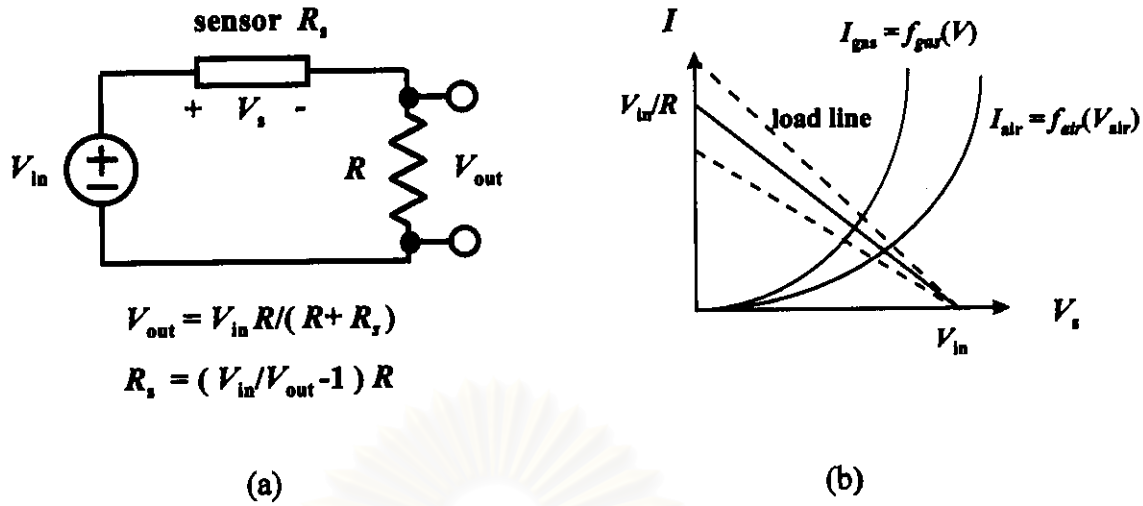

Fig. 4.2 (a) Schematic diagram of the conventional circuit and (b) *I-V* characteristic of gas sensors and load line of the conventional circuit.

4.1.2 A Novel Measuring Circuit

It was demonstrated that in the conventional measuring circuit, S depends on two parameters, i.e., R and V_{in}. To overcome this problem, an alternative circuit was designed. The schematic diagram of the proposed circuit is shown in Fig. 4.3, *I-V* characteristic of gas sensor and load line of the new circuit are also sketched in the same figure. The operation of this circuit is indeed similar to the constant voltage circuit. The load lines of this circuit are represented by the vertical lines in Fig. 4.3(b). The voltage across gas sensor is always constant ($V_s = V_{in}$) under all circumstance. The current through gas sensor is converted to the voltage signal by using an Op-amp and a resistor, R. The relation of V_{out} and R_s can be derived as follows.

$$V_{out} = -IR = -V_{in}\frac{R}{R_s} \tag{4.9}$$

$$R_s = -\frac{V_{in}}{V_{out}}R \tag{4.10}$$

From eq. (4.9), the sensor sensitivity can be obtained directly from the ratio of the output voltage in air to the output voltage in gas.

$$S = \frac{R_{air}}{R_{gas}} = \frac{V_{out\ in\ gas}}{V_{out\ in\ air}} \tag{4.11}$$

Any change in R has no effect in the calculation of the sensor resistance and also sensitivity. The vertical load line in Fig. 4.3(b) means that the electrical operating point of gas sensor is controlled only by the external voltage source. It should be noticed that there is no term of R and V_{in} remaining exist in eq. (4.11), thus they seem to have no effect on the calculation of sensor sensitivity. However, S is still depend on V_{in}, we can derive an alternative form of S in terms of V_{in}, C and α using the I-V relation in eq. (4.6).

$$S = \frac{C_{gas}}{C_{air}} V_{in}^{(\alpha_{gas} - \alpha_{air})} \tag{4.12}$$

By setting $V_{air} = V_{gas} = V_{in}$ in eq. (4.7), we will come to the same result. It is obvious that from eq. (4.12), S depends only on V_{in}. In practice, the gas sensing is performed at a constant bias voltage. Therefore, if the voltage source of all gas sensors is set to the same value, S from different sensors can be compared quantitatively.

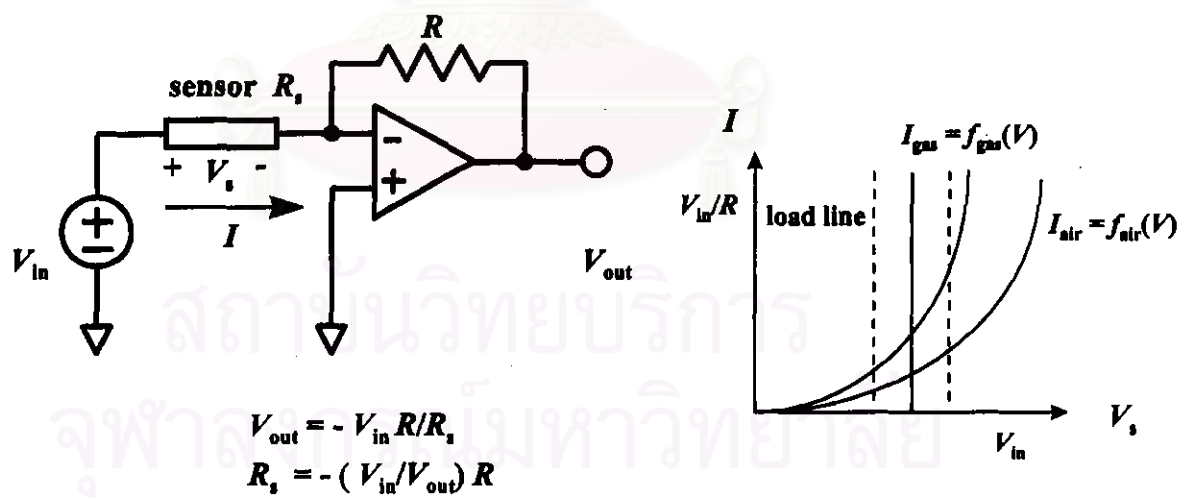

Fig. 4.3 (a) Schematic diagram of the novel measuring circuit and (b) I-V characteristic of gas sensors and load line of the measuring circuit.

4.2 Experiments

In this section, the experiments had been designed and done to evaluate the analytical results in previous section. The gas measuring system described in chapter III, was used in the experiments. The conditions used in the experiments are shown in Table 4.1.

Table 4.1 Conditions for investigating the effect of series resistance on sensitivity and recovery time

Parameters	
V_{in}	5 V
R	1 kΩ to 10 MΩ
Operating temperature	300°C
Gas sensors	SnO_2 thick film gas sensors sintered at 300, 400, 500 and 600°C
Flow rate of carrier gas	400 ml/min (O_2 80 ml/min and N_2 320 ml/min)
Test sample	methyl alcohol 0. 1 % by volume
Injection volume	2 µl

4.2.1 Preparation of SnO_2 Thick Film Gas Sensors

SnO_2 powder was prepared from tin tetrachloride ($SnCl_4$) by the co-precipitated technique[30,45]. $SnCl_4$ aqueous solution was neutralized by ammonia solution (30%). This resulted in precipitating of stannic acid. Then, the precipitated powder was washed thoroughly with DI water to remove NH_4^+ and Cl^- ion. This powder was calcined at 80°C for 24 h and followed by sintering at temperature of 300, 400, 500 and 600°C for 3 h. The diagram for the SnO_2 powder preparation is summarized in Fig. 4.4. Finally, SnO_2 powder was painted on glass substrates with two Ti/Pt electrodes. The electrodes were prepared by electron beam evaporator. The thickness of Ti and Pt was 500 and 1000 Å respectively. The space between

electrodes was 1 mm. Fig 4.5 shows the structure of the fabricated sensors. Fig. 4.6 shows the specified surface area of SnO_2 powder sintered at different temperature measured for the BET method. In Figure 4.6 also shows the estimated grain size, D_{av} calculated from the surface area, S_{av} using eq. (4.13).

$$D_{av} = \frac{6}{d \cdot S_{av}} \tag{4.13}$$

where d is the density of SnO_2 = 6.95 g/cm^3. This equation is based on the assumption that SnO_2 particle has spherical shaped. From Fig. 4.6, it is clear that the specific surface area decreased as the sintering temperature increased. While the estimated grain size showed the opposite change.

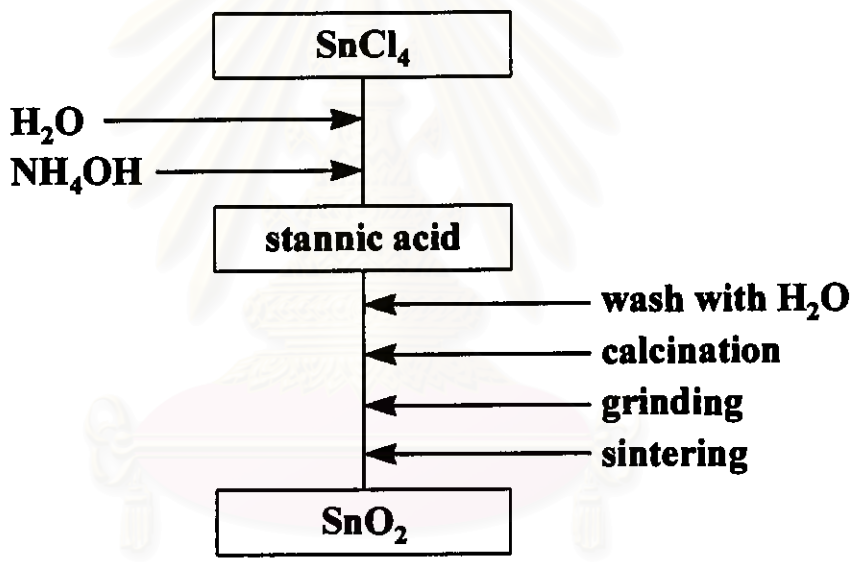

Fig. 4.4 Diagram for SnO_2 preparation

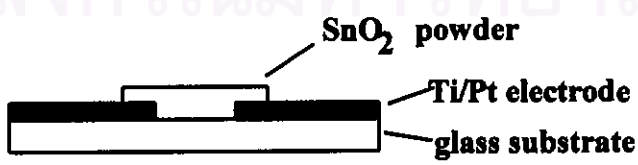

Fig. 4.5 Structure of thick film gas sensor.

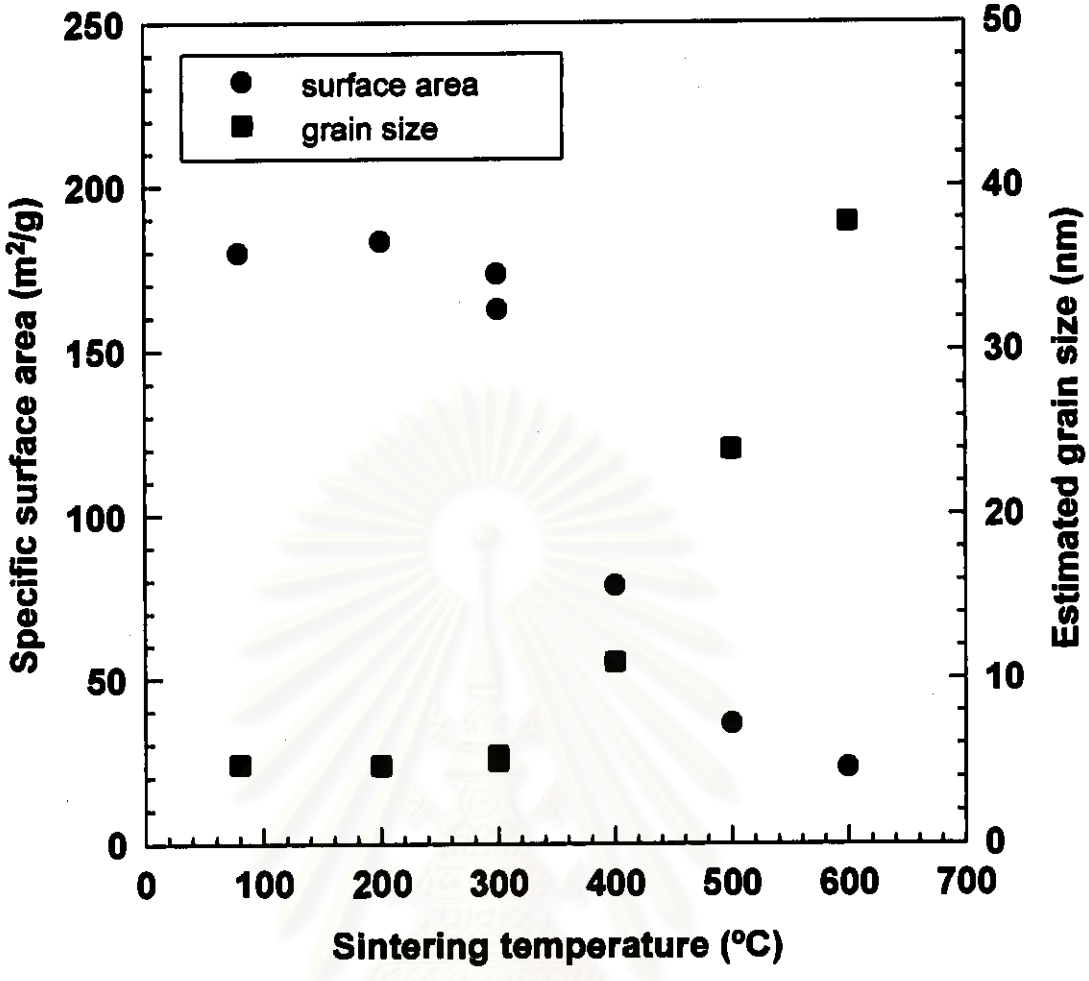

Fig. 4.6 Specified surface area and estimated grain size of SnO_2 powder as a function of the sintering temperature.

4.3 Results and Discussions

Fig. 4.7 shows typical response curves of the sensor obtained from the conventional measuring circuit and the proposed circuit. The abrupt changes of the voltage signal represents the points which gas samples were introduced to the gas measuring system.

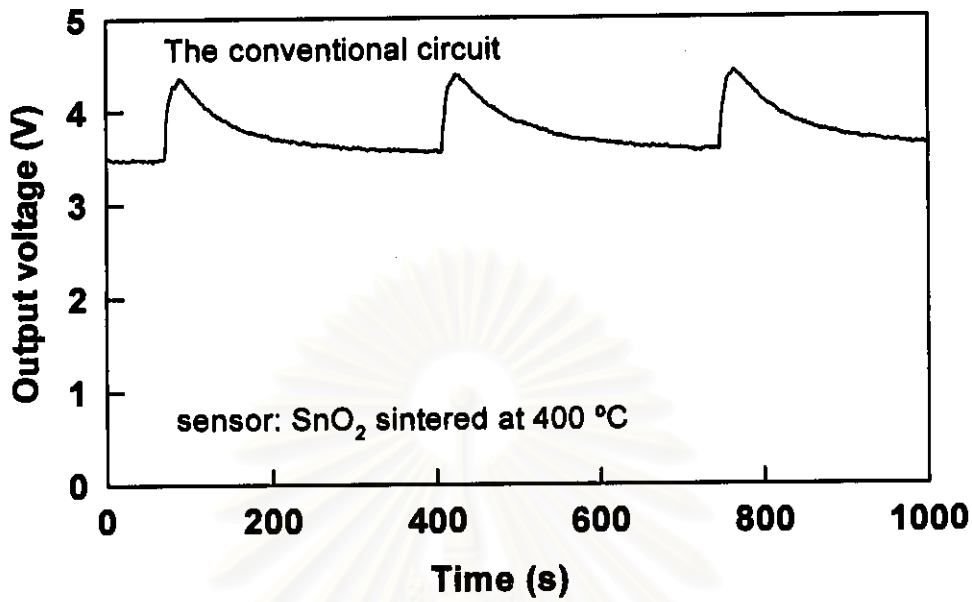

(a)

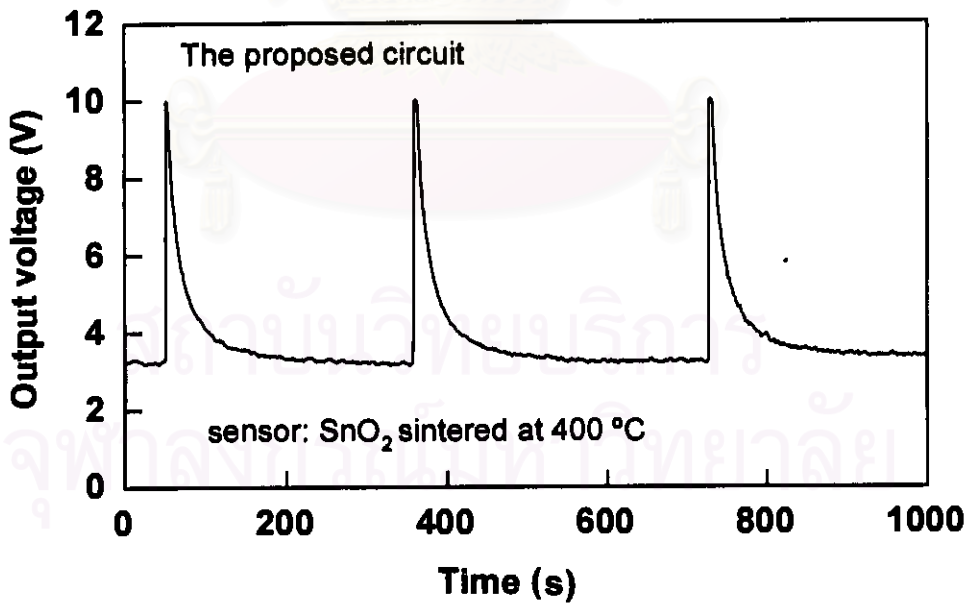

(b)

Fig. 4.7 Typical response curves obtained from (a) the conventional measuring circuit and (b) the proposed circuit.

4.3.1 The Effect of Series Resistance on Sensitivity

The change of sensitivity with resistance in the conventional circuit and the proposed circuit are demonstrated in Fig. 4.8. In the conventional circuit, we could classify gas sensors in two main groups according to the experimental results. The first group was SnO_2 gas sensors sintered at 300 and 400°C and the other group was the sensor sintered at 500 and 600°C. In the first group, sensitivity of these sensors was nearly constant without depending on the series resistance. While, sensitivity of the later group increased monotonically, as resistance decreased. It can be seen from Fig. 4.8(a) that in the conventional circuit, the calculated sensitivities may have different values up to five or six folds. This difference made the conventional circuit not suitable for comparing the gas sensing performance quantitatively.

To explain these phenomena, the calculation procedure in the section 4.1.1 was utilized. Table 4.2 shows C and α parameter of the gas sensors in air and gas ambient. The values of both parameters were calculated from *I-V* characteristics. Examples of *I-V* characteristics of the sensor that was sintered at 600?C are given in Fig. 4.9. By using values in Table 4.2 and eq. (4.3), S in term of R was solved numerically using Newton-Raphson method. The solid lines in Fig. 4.7(a) represent the results of the calculations. The results fitted quite well with the experimental data. It should be noticed that α of all sensors was greater than 1. This implied that all sensors possess the non-linear I-V characteristics. Moreover, it is clear that the dependence of S on R is determined mainly by α parameter.

In the proposed circuit, S of all sensors was nearly constant with the independence to the resistive component in the circuit. The results are shown in Fig. 4.8(b). Although, 300°C SnO_2 showed a decrease of S at very low resistance. The solid line in Fig 4.8(b) is calculated from eq. (4.12) and the values shown in Table 4.2. Although, the experimental data form 500 and 600°C gas sensor exhibited some difference from the calculated results, , they showed the same trend predicted by eq. (4.12).

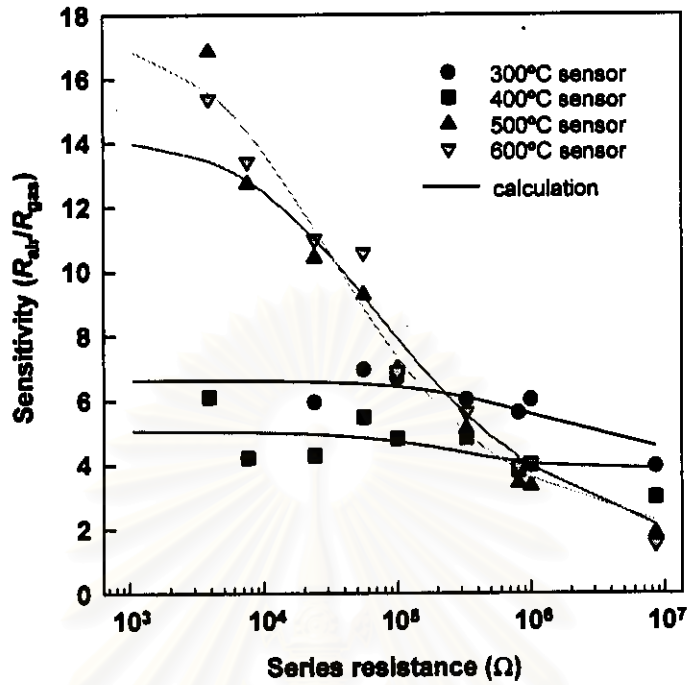

(a)

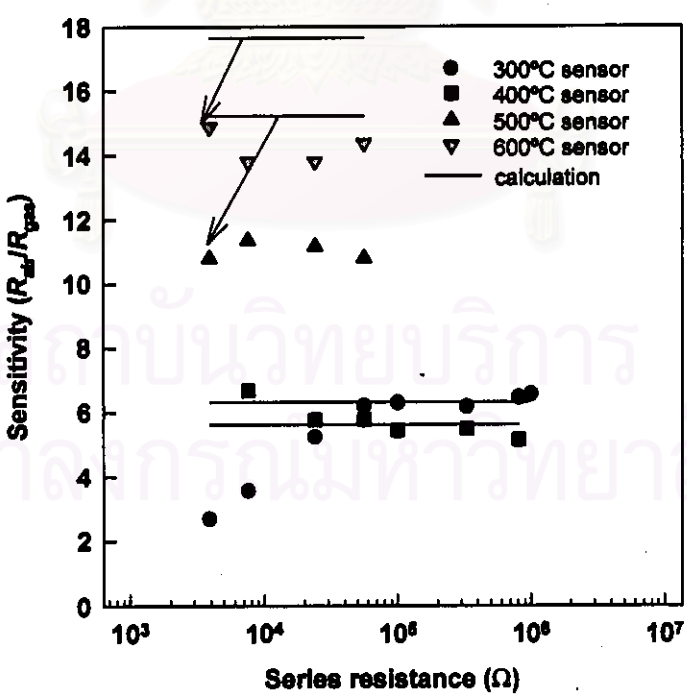

Fig. 4.8 Comparison of the effect of R on S in (a) the convention circuit and (b) the proposed circuit.

Table 4.2 Summary of C and α in air and gas ambient of the gas sensors used in the experiments.

sensor	*I-V* in air		*I-V* in gas	
	C	α	C	α
300°CSnO_2	1.5×10^{-7}	1.236	9.3×10^{-7}	1.248
400°CSnO_2	1.3×10^{-7}	1.784	1.0×10^{-6}	1.519
500°CSnO_2	9.9×10^{-7}	1.218	5.6×10^{-6}	1.833
600°CSnO_2	3.9×10^{-7}	1.780	2.3×10^{-6}	2.461

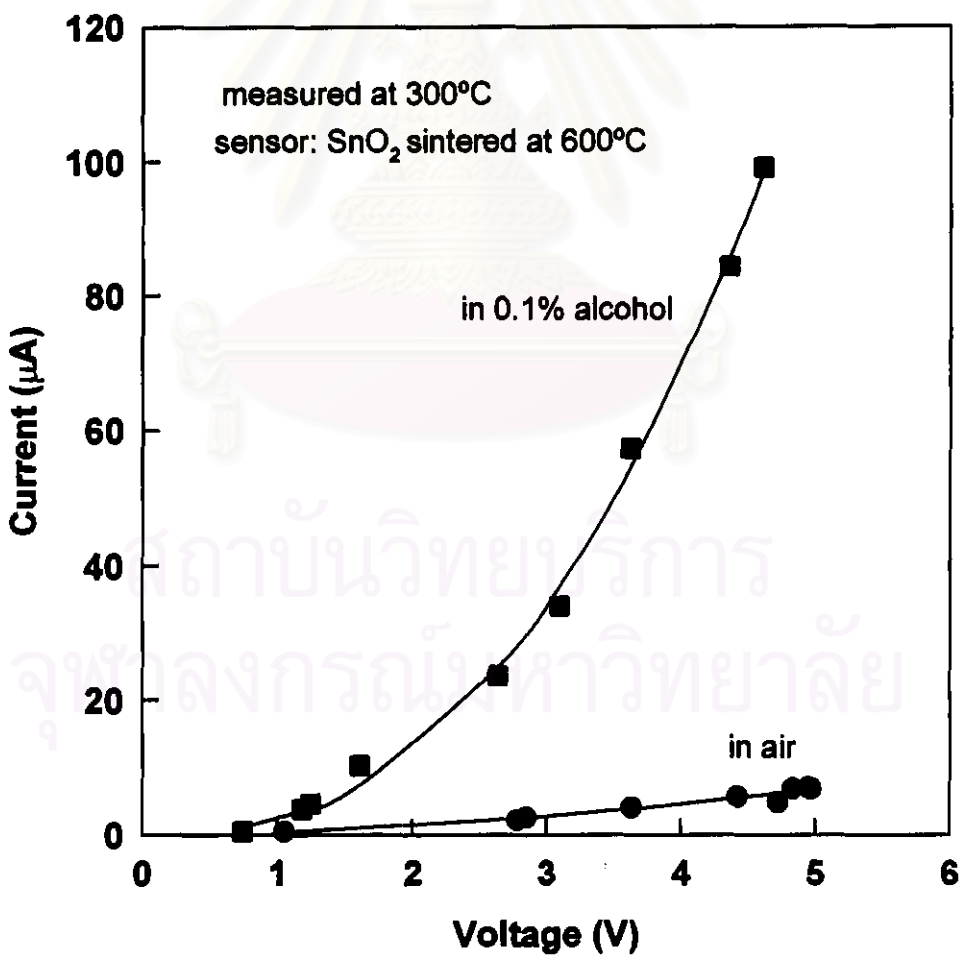

Fig. 4.9 Example of *I-V* characteristic of gas sensor

4.3.2 The Effect of Series Resistance on Recovery Time

We also investigated the effect of the series resistance on recovery time and the results are shown in Fig. 4.10. It was clear that in the conventional circuit, all SnO_2 sensors exhibited an increase of recovery time with series resistance. While, in the case of our proposed circuit, the variations of recovery time with the resistive component could not be observed (Fig. 4.10(b)). Moreover, recovery time of the proposed circuit were lower than that of the conventional circuit.

At the present state, we could not explain this phenomena theoretically. However, by considering the capacitance of the depletion layer at the grain boundary, it is reasonable to assume that the simplified dynamic model of gas sensors could be represented by a resistance connecting in parallel with a capacitance. The measuring circuits including the dynamic model of gas sensors are shown in Fig. 4.11. Here, we divided the parameters contributing to sensor recovery time, t_r.

The conventional circuit:

$$t_r \propto \tau_1 + \tau_2 \tag{4.14}$$

The proposed circuit:

$$t_r \propto \tau_1 \tag{4.15}$$

where, τ_1 is the time constant involving the chemical reaction of oxygen readsorption on SnO_2 surface after its reaction with alcohol (in this case). τ_2 is the time constant of discharging through the parallel resistance of $R// R_s$ and C_s or $\tau_2 \propto (R//R_s)C_s$.

It is clear that in the case of the conventional circuit, there was an additional term, i.e., τ_2, contributing to the recovery time. This term increased with the value of the external resistance, this is consistent with the experimental results (Fig. 4.10(a)).

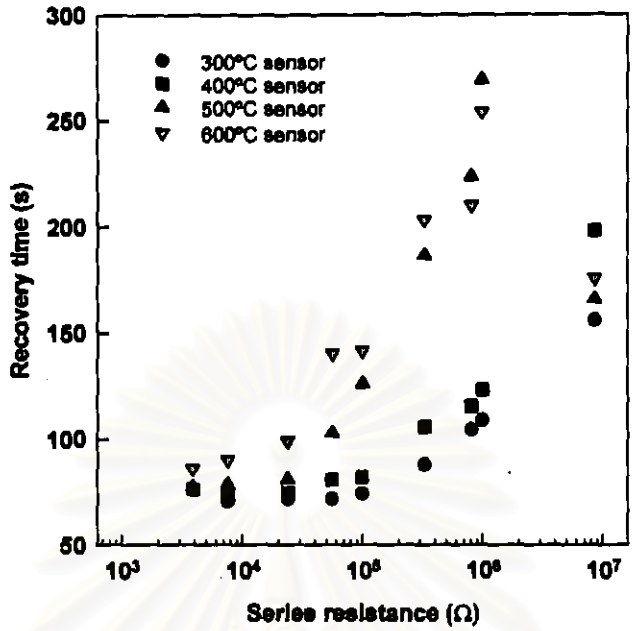

(a)

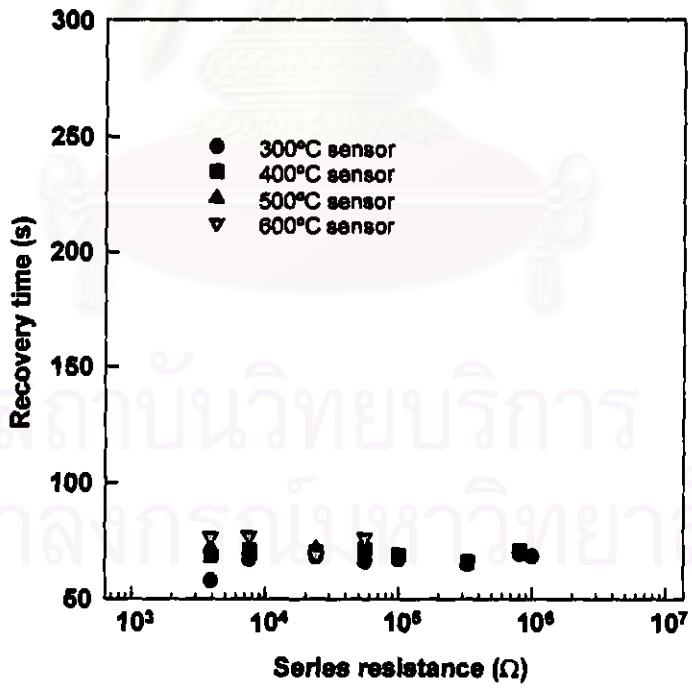

(b)

Fig. 4.10 Comparison of the effect of series resistance on recovery time in (a) the convention circuit and (b) the proposed circuit.

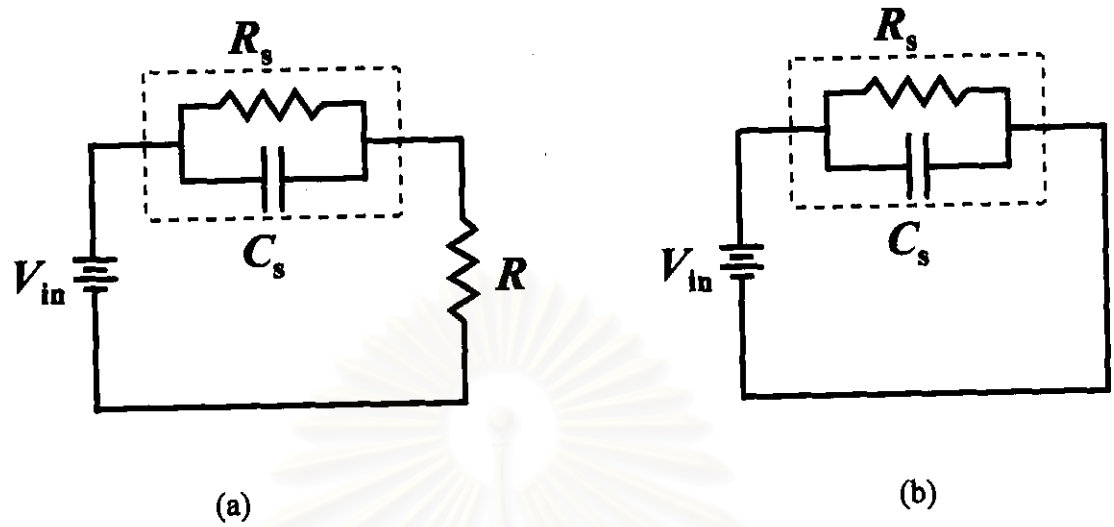

(a) (b)

Fig. 4.11 Equivalent circuit for (a) the conventional circuit and (b) the proposed circuit.

In the case of the proposed circuit, $V_s = V_{in}$ or the voltage of a gas sensor is constant all the time, therefore there is no effect of the electrical time constant of R_sC_s. Consequently, the recovery time is constant and independent to the variation of the external resistance and the electrical properties of gas sensors (Fig. 4.10(b)). This means the time constant of the pure chemical reaction between gas and semiconductors.

It should be remarked that in the proposed circuit, gas sensor is biased at a fixed voltage, therefor τ_1 of eq. (4.15) is constant and not dependent on the external resistance as shown in Fig. 4.10(b). It is noted that the important features of the curves in Fig. 4.10(a) are an asymptotic approach to constant recovery time at very low external resistance and an increase of recovery time with the values of external resistance. At very low external resistance, we can approximate that in eq. (4.14), $\tau_1 >> \tau_2$, this results in the constant recovery time in this region and the recovery time of the conventional circuit are comparable to that of the proposed circuit. From the circuit view point, the operating point of gas sensor in this region is equivalent to the operating point of gas sensor in the proposed circuit (cf. Section 3.5).

4.3.3 The Effect of Bias Voltage in the Proposed Circuit.

In the previous section, it has been demonstrated that the values of resistance, R has no effect on sensitivity in the proposed circuit. However, the effect of bias voltage, V_{in} still exists. In the section 4.1.2, S has been derived in term of V_{in} as shown in eq. (4.12). The experimental results are shown in Fig. 4.12. Fig. 4.12 also shows the variations of recovery time with bias voltage. The changes of S with V_{in} could be well described using eq. (4.12). While, the decrease of recovery time with V_{in} indicated the voltage across gas sensor assist the adsorption process of oxygen on the surface of gas sensors.

4.4 Comparison of the Conventional Circuit and the Proposed Circuit in the Other Aspects

4.4.1 Sensitivity

The output voltage of the conventional and the proposed circuit can not exceed the supplied voltage of the Op-amp. In this work, the dual-polarity power supply of ±12 V was used. However, A/D converter has a limiting input at ±10 V. Thus, the maximum output voltage is 10 V. We can calculate the maximum sensitivity of the proposed circuit in terms of $V_{out\ in\ air}$ or R_{air} as shown in eq.(4.17).

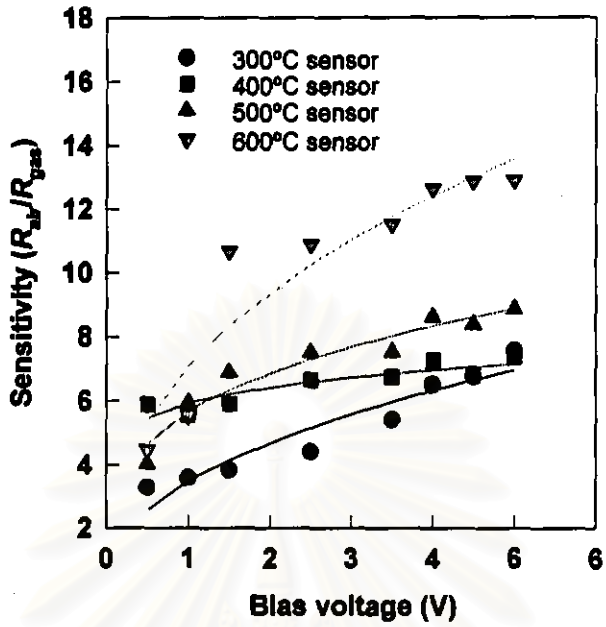

(a)

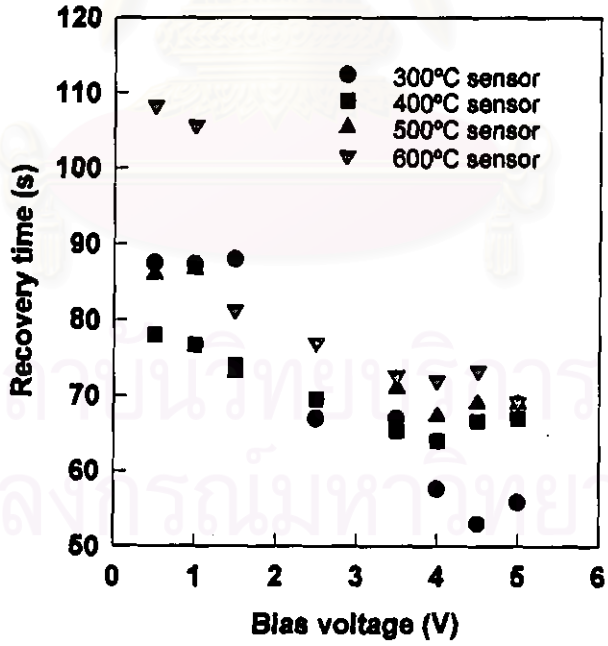

(b)

Fig. 4.12 Effect of V_{in} in our proposed circuit on (a) S and (b) recovery time.

$$S = \frac{10}{V_{\text{out in air}}} = \frac{10}{V_{\text{in}} \dfrac{R}{R_{\text{air}}}} \tag{4.17}$$

Fig. 4.13 shows the maximum sensitivity of the proposed circuit, when V_{in} = 5 V. It is obvious that to obtain a high sensitivity, one must reduce $V_{\text{out in air}}$ down to the very small value which may be under the detection limit of an A/D converter. This will cause a large error in the calculation of sensitivity as will be shown later. This means that this circuit is not suitable to a very high sensitivity gas sensor which is greater than 100. Whereas, in the convention circuit does not show such the limitation in the calculation of sensitivity. The relation of S and $V_{\text{out in gas}}$ for both circuit is shown in Fig. 4.14. However, a large error will occur in the regions of very low and high output voltage, this will be discussed in the section 4.4.2.

We can modify the proposed circuit to measure a very high sensitivity. This can be achieved by replacing the resistive element with an diode or transistor as shown in Fig. 4.15. The relation of S and V_{out} are given as follows.

[Theoretical] $$V_{\text{out}} = -\frac{kT}{q}\ln\left(\frac{I + I_{\text{o}}}{I_{\text{o}}}\right) \approx -\frac{kT}{q}\ln\left(\frac{V_{\text{in}} / R_{\text{s}}}{I_{\text{o}}}\right) \tag{4.18}$$

[Empirical] $$V_{\text{out}} \approx -\frac{kT}{q}\ln\left(CV^{\alpha}\right) \approx -\frac{kT}{q}\ln C - \frac{kT}{q}\alpha \ln V_{\text{in}} \tag{4.19}$$

$$V_{\text{out in gas}} - V_{\text{out in air}} = \frac{kT}{q}\ln\left(\frac{R_{\text{air}}}{R_{\text{gas}}}\right) = \frac{kT}{q}\ln(S) = \frac{kT}{q}\ln\left(\frac{C_{\text{gas}}}{C_{\text{air}}} V_{\text{in}}^{(\alpha_{\text{gas}} - \alpha_{\text{air}})}\right) \tag{4.20}$$

This circuit still keeps the advantage of the previous designed circuit, in addition, it is clear from eq. (4.19) by plotting $V_{out\ in\ air}$ or $V_{out\ in\ gas}$ versus $\ln(V_{in})$, the straight line should be obtained. The slope gives the non-linear coefficient, α in air or gas, and the intercept, $\ln(V_{in}) = 0$ gives C in air or in gas.

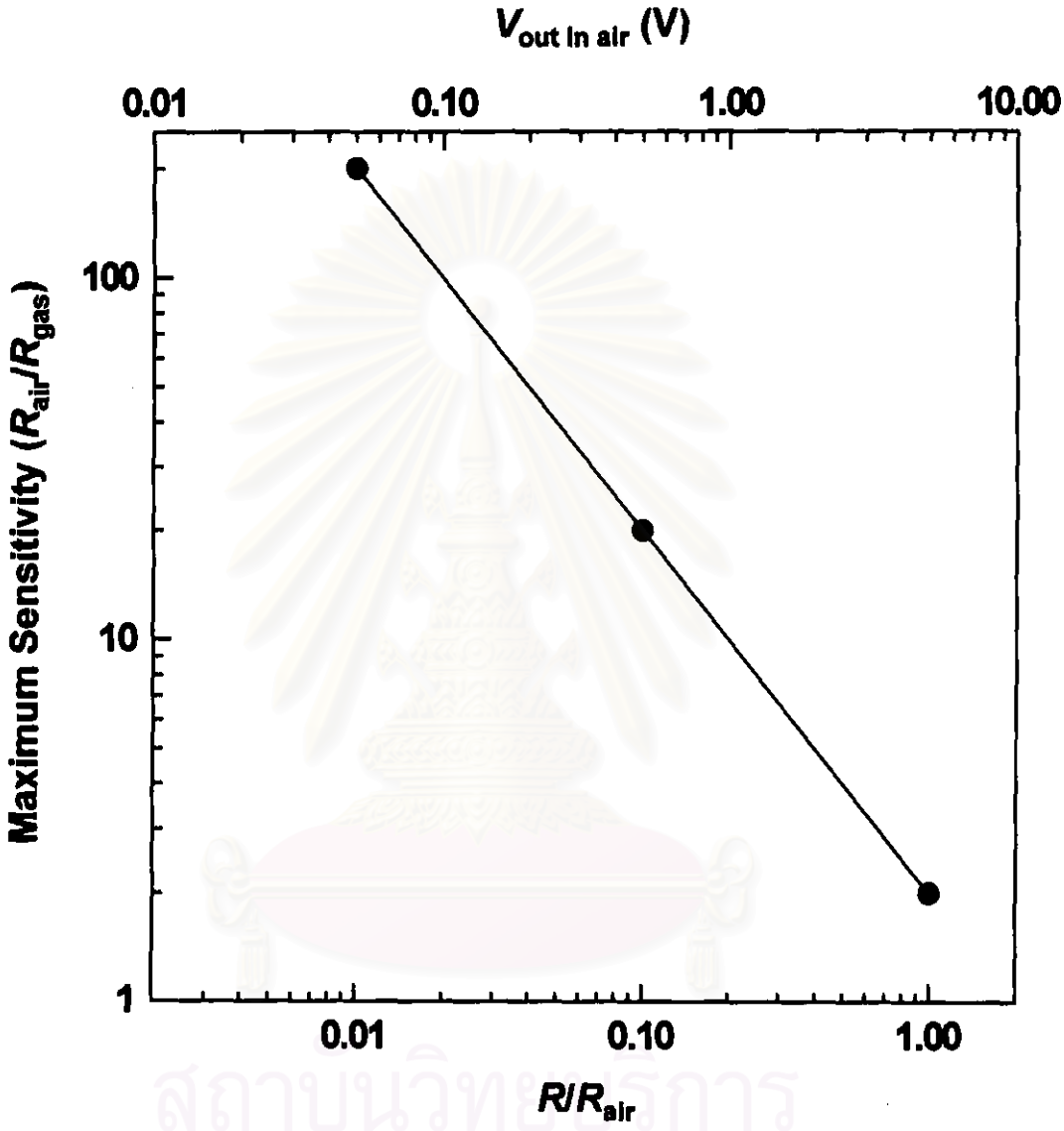

Fig. 4.13 Maximum sensitivity of the proposed circuit at $V_{in} \approx 5$ V.

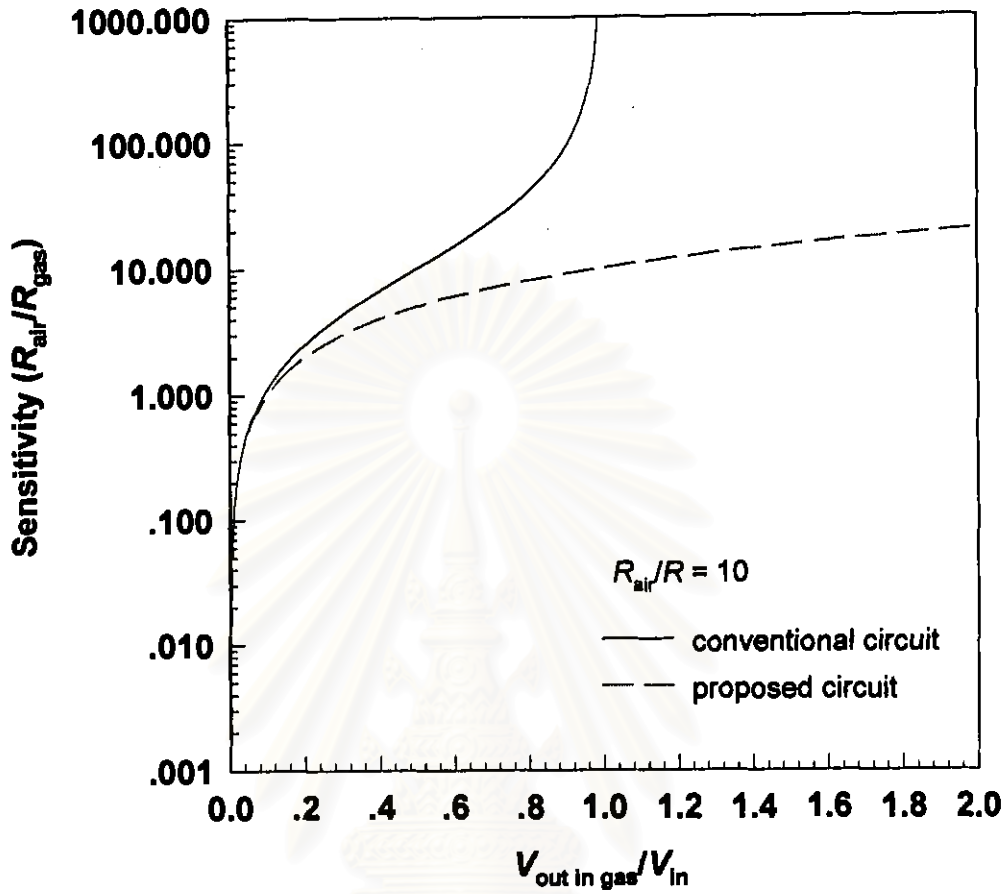

Fig. 4.14 Relationship between S and $V_{out\ in\ gas}$ at $R_{air}/R = 10$.

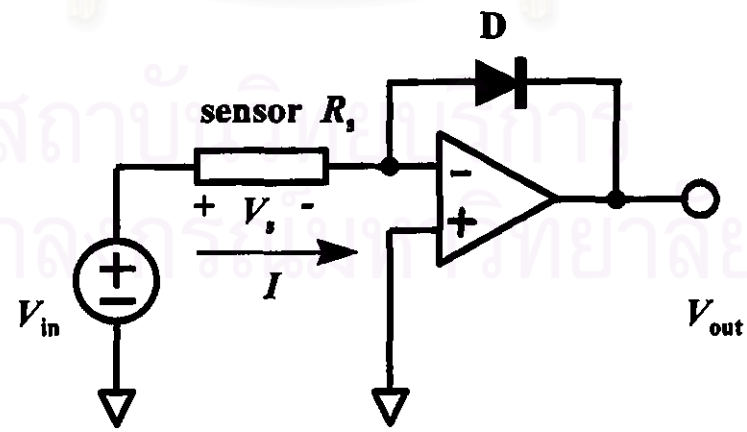

Fig. 4.15 Schematic diagram of the modified circuit to measure a high sensitivity gas sensor.

4.4.2 Error in the Calculation of Sensitivity

Error in the calculation of sensitivity is determined by the error in evaluations of resistance in air and gas ambient. This is demonstrated in eq. (4.20)

$$\frac{dS}{S} = \frac{dR_{air}}{R_{air}} - \frac{dR_{gas}}{R_{gas}} \tag{4.20}$$

We can show that this error in both circuit can be expressed as follows.

For the conventional circuit:

$$\frac{dS}{S} = -\left[\frac{(V_{in}/V_{out\ in\ air})^2}{(V_{in}/V_{out\ in\ air}-1)}\right]\frac{dV_{out\ in\ air}}{V_{in}} + \left[\frac{(V_{in}/V_{out\ in\ gas})^2}{(V_{in}/V_{out\ in\ gas}-1)}\right]\frac{dV_{out\ in\ gas}}{V_{in}} \tag{4.21}$$

For the proposed circuit:

$$\frac{dS}{S} = -\frac{dV_{out\ in\ air}}{V_{out\ in\ air}} + \frac{dV_{out\ in\ gas}}{V_{out\ in\ gas}} \tag{4.22}$$

By considering the forms of the above equations, it was found that the total error in the case of the conventional circuit is a complex function. While, in the case of the proposed circuit, the total error is only equal to the summation of an error occurring in measuring voltage signals in air and gas.

If we use a 12-bit A/D converter to measure voltage signal in the range of 0-10 V. The resolution is 10/4095 V. Therefor, the error in measuring a voltage signal is equal to ± 1 bit or ±10/4095 V. By using these values, we can plot the relation of the total error in both circuits as shown in Fig. 4.16. It is clear that for the conventional circuit, a large error in the determination of sensitivity will occur in the region of very low and high output voltage. While, a large error in the proposed circuit only occur in the region of very low voltage. In order to guarantee the error of A/D conversion in the acceptable limit (≤ 10%), it should not do the experiments at very low output voltage.

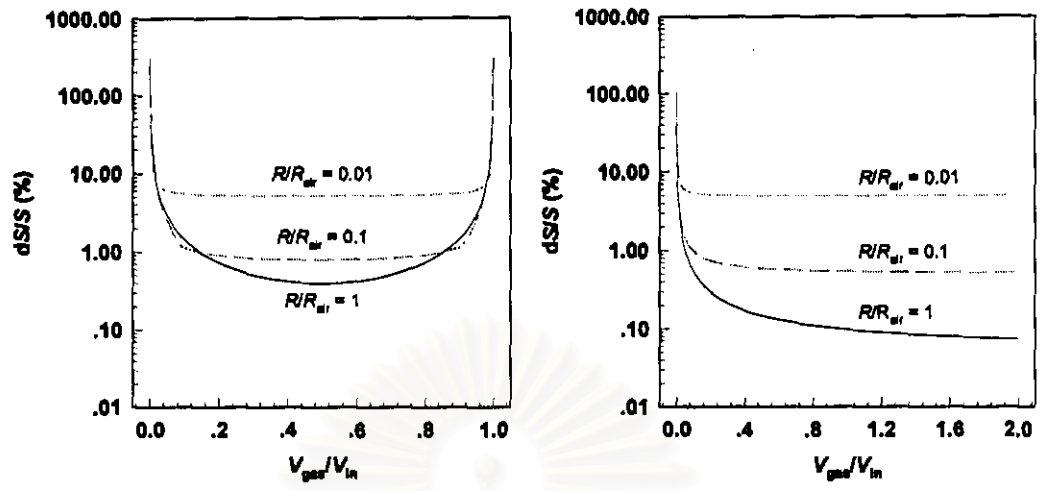

Fig. 4.16 Error in determination of sensitivity in (a) the conventional circuit and (b) the proposed circuit.

4.5 Summary

In this chapter, we have shown that the systematic analysis of the measuring circuits by considering the *I-V* characteristics of gas sensors can predict the effect of the circuit components on the gas sensing parameter, i.e., sensitivity. Although, in the point involving the recovery time, the theoretical explanation is still unsolved. The developed circuit is valuable to comparing of the gas sensing performance from various gas sensors . In summary, we concluded the performance of the conventional circuit and the proposed circuit in various aspects as illustrated in Table 4.3.

Table 4.3 Comparison between the conventional circuit and the proposed circuit.

The conventional circuit	The proposed circuit
(1) G_s or R_s is a non-linear function of V_{out}	(1) G_s is a linear function of V_{out}
(2) S is a complex function of V_{out}	(2) S is a simple function of V_{out}
(3) S depends on V_{in} and R	(3) S depends on V_{in} only
(4) dS/S is a complex function	(4) dS/S is the summation of the error in measuring voltage in air and gas
(5) Hardly to be used to compare the sensing performance of gas sensors	(5) Can be used to compare the sensing performance of gas sensors
(6) Recovery time depends on R	(6) Recovery time does not depend on R and faster